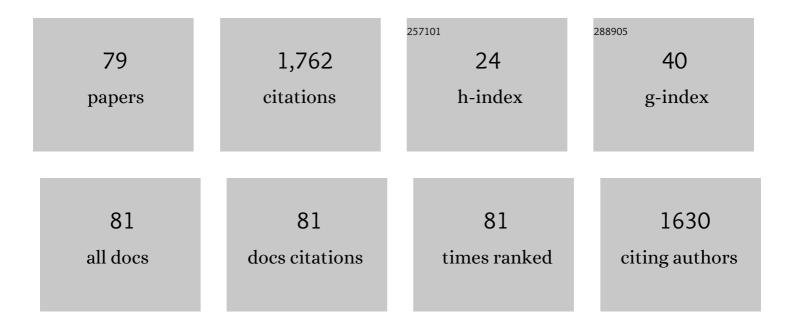
Asami Sano-Furukawa

List of Publications by Year in descending order

Source: https://exaly.com/author-pdf/3186216/publications.pdf Version: 2024-02-01



#	Article	IF	CITATIONS
1	Suppressed Lattice Disorder for Large Emission Enhancement and Structural Robustness in Hybrid Lead Iodide Perovskite Discovered by Highâ€Pressure Isotope Effect. Advanced Functional Materials, 2021, 31, 2009131.	7.8	20
2	Crystal structure of nesquehonite, MgCO ₃ ·3H(D) ₂ O by neutron diffraction and effect of pH on structural formulas of nesquehonite. Journal of Mineralogical and Petrological Sciences, 2021, 116, 96-103.	0.4	6
3	Observation of Dihydrogen Bonds in High-Pressure Phases of Ammonia Borane by X-ray and Neutron Diffraction Measurements. Inorganic Chemistry, 2021, 60, 3065-3073.	1.9	11
4	Halide Perovskites: Suppressed Lattice Disorder for Large Emission Enhancement and Structural Robustness in Hybrid Lead Iodide Perovskite Discovered by Highâ€Pressure Isotope Effect (Adv. Funct.) Tj ETQq	0 0 1 2 s gBT	/Overlock 10
5	Origin of magnetovolume effect in a cobaltite. Physical Review B, 2021, 103, .	1.1	3
6	Behavior of light elements in iron-silicate-water-sulfur system during early Earth's evolution. Scientific Reports, 2021, 11, 12632.	1.6	4
7	High-pressure and high-temperature neutron-diffraction experiments using Kawai-type multi-anvil assemblies. High Pressure Research, 2021, 41, 65-74.	0.4	5
8	Neutron diffraction study of hydrogen site occupancy in Fe _{0.95} Si _{0.05} at 14.7 GPa and 800 K. Journal of Mineralogical and Petrological Sciences, 2021, 116, 309-313.	0.4	2
9	Crystalline Fully Carboxylated Polyacetylene Obtained under High Pressure as a Li-Ion Battery Anode Material. Journal of Physical Chemistry Letters, 2021, 12, 12055-12061.	2.1	7
10	Distance-Selected Topochemical Dehydro-Diels–Alder Reaction of 1,4-Diphenylbutadiyne toward Crystalline Graphitic Nanoribbons. Journal of the American Chemical Society, 2020, 142, 17662-17669.	6.6	23
11	Multi-methodical study of the Ti, Fe2+ and Fe3+ distribution in chevkinite-subgroup minerals: X-ray diffraction, neutron diffraction, 57Fe Mössbauer spectroscopy and electron-microprobe analyses. Physics and Chemistry of Minerals, 2020, 47, 1.	0.3	3
12	Crystal and Magnetic Structures of Double Hexagonal Close-Packed Iron Deuteride. Scientific Reports, 2020, 10, 9934.	1.6	6
13	Anomalous hydrogen dynamics of the ice VII–VIII transition revealed by high-pressure neutron diffraction. Proceedings of the National Academy of Sciences of the United States of America, 2020, 117, 6356-6361.	3.3	17
14	Practical effects of pressure-transmitting media on neutron diffraction experiments using Paris–Edinburgh presses. High Pressure Research, 2020, 40, 325-338.	0.4	4
15	Structure refinement of black phosphorus under high pressure. Journal of Chemical Physics, 2020, 153, 014704.	1.2	9
16	Developments of nano-polycrystalline diamond anvil cells for neutron diffraction experiments. High Pressure Research, 2020, 40, 184-193.	0.4	16
17	Crystal structure and magnetism of MnO under pressure. Physical Review B, 2020, 101, .	1.1	4
18	lce Ic without stacking disorder by evacuating hydrogen from hydrogen hydrate. Nature Communications, 2020, 11, 464.	5.8	50

#	Article	IF	CITATIONS
19	X-ray and Neutron Study on the Structure of Hydrous SiO2 Glass up to 10 GPa. Minerals (Basel,) Tj ETQq1 1 0.784	4314 rgBT 0.8	/gverlock 1
20	Neutron diffraction study on the deuterium composition of nickel deuteride at high temperatures and high pressures. Physica B: Condensed Matter, 2020, 587, 412153.	1.3	5
21	Crystal chemistry of Sr–rich piemontite from manganese ore deposit of the Tone mine, Nishisonogi Peninsula, Nagasaki, southwest Japan. Journal of Mineralogical and Petrological Sciences, 2020, 115, 391-406.	0.4	0
22	Pressure Effect on Isotope Fractionation Factor. Review of High Pressure Science and Technology/Koatsuryoku No Kagaku To Gijutsu, 2020, 30, 85-94.	0.1	0
23	Development of a technique for high pressure neutron diffraction at 40â€GPa with a Paris-Edinburgh press. High Pressure Research, 2019, 39, 417-425.	0.4	23
24	Hexagonal Close-packed Iron Hydride behind the Conventional Phase Diagram. Scientific Reports, 2019, 9, 12290.	1.6	31
25	Interstitial hydrogen atoms in face-centered cubic iron in the Earth's core. Scientific Reports, 2019, 9, 7108.	1.6	42
26	Crystal structure change of katoite, Ca3Al2(O4D4)3, with temperature at high pressure. Physics and Chemistry of Minerals, 2019, 46, 459-469.	0.3	4
27	Structure change of monoclinic ZrO ₂ baddeleyite involving softenings of bulk modulus and atom vibrations. Acta Crystallographica Section B: Structural Science, Crystal Engineering and Materials, 2019, 75, 742-749.	0.5	9
28	Pressureâ€Induced Diels–Alder Reactions in C ₆ H ₆ ₆ F ₆ Cocrystal towards Graphane Structure. Angewandte Chemie, 2019, 131, 1482-1487.	1.6	1
29	Pressureâ€Induced Diels–Alder Reactions in C ₆ H ₆ ₆ F ₆ Cocrystal towards Graphane Structure. Angewandte Chemie - International Edition, 2019, 58, 1468-1473.	7.2	36
30	Behavior of intermolecular interactions in <i>α</i> -glycine under high pressure. Journal of Chemical Physics, 2018, 148, 044507.	1.2	9
31	High-Pressure–High-Temperature Study of Benzene: Refined Crystal Structure and New Phase Diagram up to 8 GPa and 923 K. Crystal Growth and Design, 2018, 18, 3016-3026.	1.4	20
32	Direct observation of symmetrization of hydrogen bond in δ-AlOOH under mantle conditions using neutron diffraction. Scientific Reports, 2018, 8, 15520.	1.6	48
33	Pressure-induced stacking disorder in boehmite. Physical Chemistry Chemical Physics, 2018, 20, 16650-16656.	1.3	4
34	Hydrogenation of iron in the early stage of Earth's evolution. Nature Communications, 2017, 8, 14096.	5.8	50
35	Bulk moduli and equations of state of ice VII and ice VIII. Physical Review B, 2017, 95, .	1.1	36
36	What can we do with the High-Pressure Neutron Diffractometer PLANET?. Nihon Kessho Gakkaishi, 2017, 59, 301-308.	0.0	0

#	Article	IF	CITATIONS
37	<i>In-situ</i> Neutron Diffraction of Iron Hydride in Iron-silicate-water System under High Pressure and High Temperature Condition. Hamon, 2017, 27, 104-108.	0.0	0
38	Materials and Life Science Experimental Facility (MLF) at the Japan Proton Accelerator Research Complex II: Neutron Scattering Instruments. Quantum Beam Science, 2017, 1, 9.	0.6	69
39	Phase Transitions and Polymerization of C ₆ H ₆ –C ₆ F ₆ Cocrystal under Extreme Conditions. Journal of Physical Chemistry C, 2016, 120, 29510-29519.	1.5	25
40	Partially ordered state of ice XV. Scientific Reports, 2016, 6, 28920.	1.6	31
41	Overview of High-Pressure Neutron Beamline, PLANET, and Practical Aspects of the Experiments. Review of High Pressure Science and Technology/Koatsuryoku No Kagaku To Gijutsu, 2016, 26, 89-98.	0.1	0
42	Toward the High-Pressure and Temperature Neutron Diffraction Using Large Volume Press. Review of High Pressure Science and Technology/Koatsuryoku No Kagaku To Gijutsu, 2016, 26, 99-107.	0.1	1
43	lce VII from aqueous salt solutions: From a glass to a crystal with broken H-bonds. Scientific Reports, 2016, 6, 32040.	1.6	31
44	How had the High-Pressure Neutron Diffractometer PLANET been Constructed?. Hamon, 2016, 26, 85-90.	0.0	0
45	Synthesis, Structure, and Pressure-Induced Polymerization of Li3Fe(CN)6 Accompanied with Enhanced Conductivity. Inorganic Chemistry, 2015, 54, 11276-11282.	1.9	6
46	Design and performance of high-pressure PLANET beamline at pulsed neutron source at J-PARC. Nuclear Instruments and Methods in Physics Research, Section A: Accelerators, Spectrometers, Detectors and Associated Equipment, 2015, 780, 55-67.	0.7	96
47	Crystal structure of magnesium dichloride decahydrate determined by X-ray and neutron diffraction under high pressure. Acta Crystallographica Section B: Structural Science, Crystal Engineering and Materials, 2015, 71, 74-80.	0.5	19
48	Site Occupation State of Deuterium Atoms in fcc Fe. Hamon, 2015, 25, 26-31.	0.0	0
49	Six-axis multi-anvil press for high-pressure, high-temperature neutron diffraction experiments. Review of Scientific Instruments, 2014, 85, 113905.	0.6	62
50	Site occupancy of interstitial deuterium atoms in face-centred cubic iron. Nature Communications, 2014, 5, 5063.	5.8	67
51	Observation of pressure-induced phase transition of Ĩ-AlOOH by using single-crystal synchrotron X-ray diffraction method. Physics and Chemistry of Minerals, 2014, 41, 303-312.	0.3	38
52	Phase transitions and hydrogen bonding in deuterated calcium hydroxide: High-pressure and high-temperature neutron diffraction measurements. Journal of Solid State Chemistry, 2014, 218, 95-102.	1.4	12
53	Formation of NaCl-type Lanthanum Monohydride under High Pressure. Hamon, 2013, 23, 131-136.	0.0	0
54	Formation of NaCl-Type Monodeuteride LaD by the Disproportionation Reaction of <mml:math xmlns:mml="http://www.w3.org/1998/Math/MathML" display="inline"><mml:msub><mml:mi>LaD</mml:mi><mml:mn>2</mml:mn></mml:msub>. Physical Review Letters, 2012, 108, 205501.</mml:math 	2.9	24

#	Article	IF	CITATIONS
55	Neutron powder diffraction of small-volume samples at high pressure using compact opposed-anvil cells and focused beam. Journal of Physics: Conference Series, 2012, 377, 012013.	0.3	8
56	Compression behaviors of distorted rutile-type hydrous phases, MOOH (MÂ=ÂGa, In, Cr) and CrOOD. Physics and Chemistry of Minerals, 2012, 39, 375-383.	0.3	19
57	Neutron Diffraction Study on Hydrogen Bond in Mineral in the Deep Earth. Hamon, 2012, 22, 162-165.	0.0	Ο
58	The crystal structure of Â-Al(OH)3: Neutron diffraction measurements and ab initio calculations. American Mineralogist, 2011, 96, 854-859.	0.9	15
59	Investigation of hydrogen sites of wadsleyite: A neutron diffraction study. Physics of the Earth and Planetary Interiors, 2011, 189, 56-62.	0.7	28
60	Hydrogen motions of Mg(OD)2and Ca(OD)2at several temperatures. Acta Crystallographica Section A: Foundations and Advances, 2011, 67, C241-C241.	0.3	0
61	Effects of Mg and Si ions on the symmetry of δ-AlOOH. Physics and Chemistry of Minerals, 2011, 38, 727-733.	0.3	15
62	Pressure responses of portlandite and H–D isotope effects on pressure-induced phase transitions. Physics and Chemistry of Minerals, 2011, 38, 777-785.	0.3	11
63	Neutron diffraction study on the pressure-induced cubic-tetragonal structural distortion in LaD2using total scattering spectrometer NOVA. Acta Crystallographica Section A: Foundations and Advances, 2011, 67, C331-C331.	0.3	Ο
64	High pressure experiments with the Engineering Materials Diffractometer (BL-19) at J-PARC. Journal of Physics: Conference Series, 2010, 215, 012023.	0.3	5
65	Infrared absorption spectra of δ-AlOOH and its deuteride at high pressure and implication to pressure response of the hydrogen bonds. Journal of Physics: Conference Series, 2010, 215, 012052.	0.3	10
66	The stability and equation of state for the cotunnite phase of TiO2 up to 70ÂGPa. Physics and Chemistry of Minerals, 2010, 37, 129-136.	0.3	60
67	A cubic-anvil high-pressure device for pulsed neutron powder diffraction. Review of Scientific Instruments, 2010, 81, 043910.	0.6	6
68	Change in compressibility of Â-AlOOH and Â-AlOOD at high pressure: A study of isotope effect and hydrogen-bond symmetrization. American Mineralogist, 2009, 94, 1255-1261.	0.9	85
69	A new high-pressure polymorph of Ti ₂ O ₃ : implication for high-pressure phase transition in sesquioxides. High Pressure Research, 2009, 29, 379-388.	0.4	33
70	Aluminous hydrous mineral <i>δ</i> â€AlOOH as a carrier of hydrogen into the coreâ€mantle boundary. Geophysical Research Letters, 2008, 35, .	1.5	103
71	Neutron diffraction study of Â-AlOOD at high pressure and its implication for symmetrization of the hydrogen bond. American Mineralogist, 2008, 93, 1558-1567.	0.9	55
72	X-ray diffraction study of high pressure transition in InOOH. Journal of Mineralogical and Petrological Sciences, 2008, 103, 152-155.	0.4	15

Asami Sano-Furukawa

#	Article	IF	CITATIONS
73	First principles prediction of new high-pressure phase of InOOH. Journal of Mineralogical and Petrological Sciences, 2008, 103, 116-120.	0.4	13
74	Neutron diffraction study of aluminous hydroxide δ-AlOOD. Physics and Chemistry of Minerals, 2007, 34, 657-661.	0.3	21
75	In situ X-ray diffraction study of the effect of water on the garnet–perovskite transformation in MORB and implications for the penetration of oceanic crust into the lower mantle. Physics of the Earth and Planetary Interiors, 2006, 159, 118-126.	0.7	13
76	Redetermination of the high-pressure modification of AlOOH from single-crystal synchrotron data. Acta Crystallographica Section E: Structure Reports Online, 2006, 62, i216-i218.	0.2	32
77	Water controls the fields of metastable olivine in cold subducting slabs. Geophysical Research Letters, 2005, 32, .	1.5	39
78	In situ X-ray observation of decomposition of hydrous aluminum silicate AlSiO3OH and aluminum oxide hydroxide d-AlOOH at high pressure and temperature. Journal of Physics and Chemistry of Solids, 2004, 65, 1547-1554.	1.9	85
79	Metastable garnet in oceanic crust at the top of the lower mantle. Nature, 2002, 420, 803-806.	13.7	89